Design of a Liquid-Crystal Dual-Polarization Reflectarray Antenna

Robert Guirado, Gerardo Perez-Palomino, Pablo de la Rosa, Eduardo Carrasco

Information Processing and Telecommunications Center (IPTC), Universidad Politécnica de Madrid, Spain

***Abstract*—This paper demonstrates for the first time a dual polarization reconfigurable reflectarray antenna based on Liquid Crystal (LC) that operates at W-band. The antenna is electrically large and is capable of independently steering the beam of two orthogonal polarizations. Two different implementations of single-layer unit cells (single resonant and multi-resonant) capable of providing suitable phase range to independently control the two RF polarizations with enough isolation have been investigated. The single resonant cell was finally used to design a complete reflectarray antenna made of 55×55 elements, for which an accurate and efficient modeling of the cells was implemented. The antenna shows 35º of 1D scanning range with 25dBi gain and a maximum SLL of -9dB in the entire range for both polarizations at 98 GHz.**

I. Introduction

In the recent years, the popularity of mm-wave planar devices using Liquid Crystal (LC) technology has experienced a rapid growth. The LC is a material whose electric permittivity tensor can be changed when a quasi-static (AC) electric field is applied through it, due to the rotation of its anisotropic rod-like molecules. In the case of reflectarray antennas and RIS, the LC allows to electronically modify the radiation pattern and, thus, to dynamically scan a beam or provide adaptive coverage to a blind zone [1]. Compared to the different existing reconfigurable technologies, LC can be used at the hundreds of GHz range (W-band and above) while being a low-cost solution, especially due to the industry readiness inherited from the optics manufacturers, where its use is widespread. Moreover, LC allows a continuous tuning and its inherent power consumption is close to zero.

Numerous LC-based reflectarray unit cells have been introduced in the last decade, with the aim of improving the performance in terms of reconfiguration bandwidth [2], achievable phase shift [3], losses [4] and temporal response [5]. However, a very limited number of reconfigurable reflectarrays with polarization-sensitive capabilities have been presented, mainly due to the difficult unit cell design and LC characterization in that case. In [6], a complex 15-layer structure containing two independent LC cavities and polarizers independently manipulates two orthogonal polarizations. However, a simple single-layer reflectarray based on LC with an independent control of each polarization in the same unit cell, and how to efficiently model it, can not be found in literature.

This work was supported by the Spanish Ministry of Science and Innovation (ENHANCE-5G PID2020-114172RB-C22) and by the Spanish Ministry for Digital Transformation and Public Function (TSI-063000-2021-83). R. Guirado acknowledges the support of a fellowship from "la Caixa" Foundation (ID 100010434). The fellowship code is LCF/BQ/DR21/11880029.

In this paper, an electrically large LC-based reflectarray antenna capable of beam-steering polarization independent beams in W-band, together with a proper modeling process, are presented. Two LC unit cells sensitive to both polarizations have been designed and evaluated. The first cell (single resonant) exhibits a phase range of 200º at 98 GHz and its structure enables introducing a simple polarization bias network. The other cell (multi-resonant) shows a complete cycle of phase-range (>360º) in a wider bandwidth, but at the expense of requiring another type of technology to implement the biasing. An accurate modeling of the LC cells, that includes the bias network to control the phase-shift of the two RF polarizations in the same cell, is proposed. Then, a complete LC reflectarray antenna is designed. The antenna is capable of independently beam-steering and focusing each polarization in one plane at least 35º with a gain of 25dBi and a sidelobe level (SLL) as low as -9 dB in the entire scanning range.

II. Dual Polarization LC Unit Cell

A. Unit Cell Design

In LC-based reflectarray unit cells, the structure consists on a stack of layers, typically one of them being the LC cavity. A common structure, from bottom to top, is the following one: a substrate supporting a metallic ground plane, the LC cavity, and a top superstrate electrode from which resonant elements protrude (see Fig. 1).

The most straightforward way to independently control different polarizations in a LC-based reflectarray element is to bias with different voltages the cavity volume beneath the resonant elements sensitive to each polarization, within the same unit cell. Since the rotation of the LC molecules is a local property throughout the cavity, this allows different regions of the same unit cell to be biased independently to achieve separate reflection coefficients for each polarization. However, that introduces a strong inhomogeneity across the transversal direction (parallel to the surface), which must be accurately modelled in a polarization-sensitive design. Nevertheless, besides difficult to achieve, a very fine-grained model of these structures is excessively computationally expensive [7], and an efficient model point which considers the trade-off between computation and accuracy must be found.

Apart from the modeling, designing a unit cell sensitive to two independent polarizations which includes a LC cavity is challenging in different aspects. In a reflectarray antenna, the different cells will have different incident angles from the feed, which can vary their reflection coefficient. To reduce this

effect, the size of the period should be minimized to achieve small sensitivities with the angle of incidence. However, when including resonant elements for each polarization, the required area to fit them increases. Another handicap appears when trying to minimize the cross-polarization effects of the cell. Together with the sensitivity to the angle of incidence, the anisotropic nature of the LC makes it difficult to maintain the cell symmetry, which further contributes to the cross-polarization. Therefore, a trade-off between period size, sensitivity to angle of incidence, and cross-polarization levels must be found.

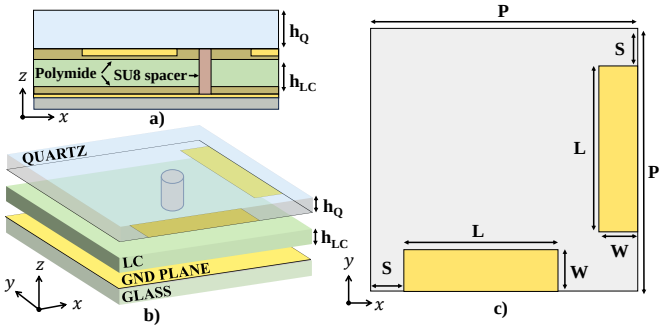

Fig. 1. a) Side view b) 3D view and c) top view of the proposed single-resonant unit cell. Dimensions (mm): $P = 1.25$, $L = 0.77$, $W = 0.15$, $S = 0.165$, $h_Q = 0.4$, $h_{LC} = 0.08$.

Considering all the aforementioned effects, two different dual-polarization LC reflectarray unit cells have been designed: one containing a single resonant element per polarization (Fig. 1), and another one containing multiple resonant elements per polarization (Fig. 2). In both cases, the chosen LC is GT7-29001 ($\varepsilon_{||} = 3.5$, $tan\delta_{||} = 0.015$ and $\varepsilon_{\perp} = 2.47$, $tan\delta_{\perp} = 0.02$ at 100 GHz), since it is specifically designed for mm-wave devices.

The unit cells consist of dipole-shaped metallic elements orthogonally oriented (along x and y considering the coordinate systems of Fig. 1 and Fig. 2). The geometry of the cell is such that the cross-polarization is minimized as much as possible. The design of the LC thickness considers a trade-off between losses and phase range. Whereas a thinner cavity increases the phase range and diminishes response time, it comes at the cost of increased losses.

Fig. 3 shows the reflection coefficient as a function of the frequency for the two polarizations (S_{XX} and S_{YY}) at incidence angle $\phi_{inc} = 0°, \theta_{inc} = 25°$. As can be seen, the multi-resonant cell exhibits a larger instantaneous bandwidth and phase range than the single-resonant cell, but since it must fit a larger number of dipoles, its period is larger and thus its tolerance to different incidence angles is much lower. Note that in the single-resonant case a relatively thick cavity ($h_{LC} = 80\mu m$) is chosen, since a single dipole resonance cannot achieve 360° phase range anyway, and this way losses are reduced and critically coupled resonances are avoided.

B. LC Bias Lines

Finally, after the RF design of the cell topology and dimensions is finished, the metallic bias lines necessary to

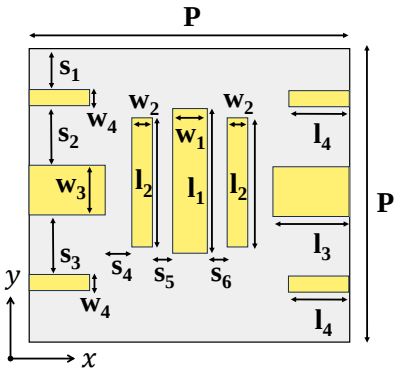

Fig. 2. Top view of the multi-resonant unit cell. Dimensions (mm): $P = 1.6$, $l_1 = 0.801$, $l_2 = 0.745$, $l_3 = 0.396$, $l_4 = 0.365$, $w_1 = 0.189$, $w_2 = 0.142$, $w_3 = 0.284$, $w_4 = 0.0945$, $s_1 = 0.16$, $s_2 = s_3 = 0.407$, $s_4 = 0.1$, $s_5 = s_6 = 0.071$, $h_Q = 0.38$, $h_{LC} = 0.056$.

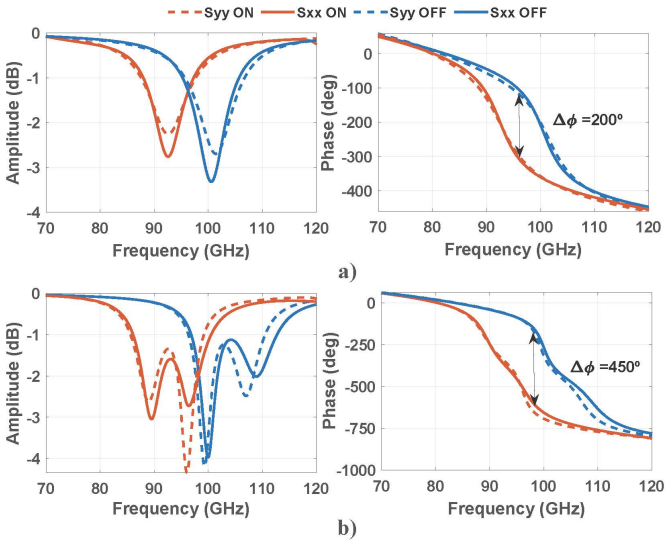

Fig. 3. Simulated amplitude and phase of the S_{XX} and S_{YY} reflection coefficients of the (a) single-resonant and (b) multi-resonant unit cells for OFF (V=0) and ON (V>>10V) states.

polarize the LC are added. This must be done carefully, as an improper placing of these lines could introduce in-band resonances and unwanted effects. In fact, in the multi-resonant cell topology, adding the LC bias lines has a very strong effect on the response, and an alternative solution (e.g. using a material which is conductive for AC signals but transparent to RF) should be used. Moreover, the complexity of this cell would also add a lot of manufacturing difficulties. Considering this and the aforementioned reasons, the focus of this work is the single-resonance unit cell reflectarray, which is enough to prove the dual polarization concept and allows to successfully scan independent beams.

In order to minimize the effect of introducing such lines in the single-resonant cell, a thorough study has been carried out (Fig. 4). Since the antenna should be able to perform scanning and focusing in a single plane, a column-like bias addressing will be used, where all the unit cells of the same column are interconnected. Several bias geometries have been analyzed and compared to the non-biased (ideal) geometry.

The finally chosen biasing geometry can be seen in Fig.

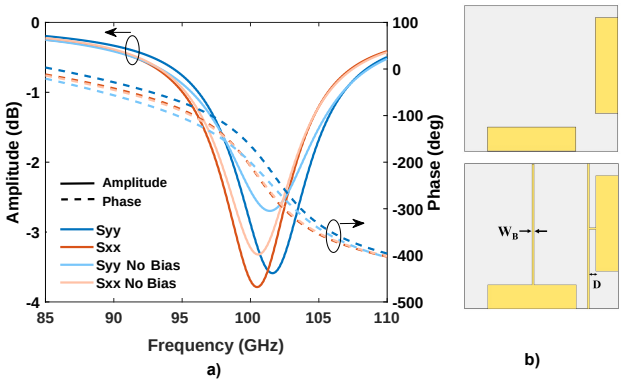

Fig. 4. Main conclusions of the analysis on the addressing bias geometry. The amplitude and phase of S_{XX} and S_{YY} are compared to the original unit cell (Vx=Vy=0V state) under oblique incidence ($\phi_{inc} = 0°, \theta_{inc} = 25°$). a) Reflection coefficient comparison. b) Ideal (top) and biased (bottom) geometries ($D = 0.06$mm, $W_b = 0.02$mm).

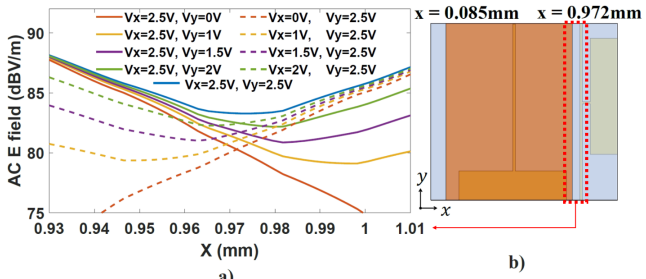

Fig. 5. a) AC electric field in the unit cell region where the bias fields of the different polarizations interact the most. The E field data is from the $y = 1.2mm$ cut (where the x bias and y bias metallization are the closest) and averaged across z. b) Resulting LC blocks for an accurate but efficient simulation.

4b. The lines connect to the dipoles orthogonally in a region where the electric field tends to be small, close to the center of the dipole. This introduces an elbow-like turn on the bias line of the y-oriented dipole, which slightly breaks the symmetry of the cell and marginally modifies S_{XX}. Nevertheless, the effects of this addressing are very limited as compared the other options, which included connecting lines continuously along y or segmenting the ground plane.

C. Unit Cell Modelling

As previously mentioned, the modelling of these structures must be done carefully. On the one hand, the LC cavity is electrically very thin, and a number of high order non-evanescent modes are excited. This makes difficult to perform an equivalent circuital analysis and forces full-wave simulations of the unit cell. Moreover, due to the presence of two different potentials in the same unit cell (one per each dipole), not only the z inhomogeneity must be accounted for, but also the $x-y$ inhomogeneity. On the other hand, using exhaustive volumetric models for the LC cavity, which can result very accurate since the LC director is precisely determined in the whole cavity, results prohibitive in a design stage due to their computation cost. To tackle the z inhomogeneity, the community has successfully used an averaging strategy of the director tilt angle in the past, which reduces the computation while assuming a very limited error [7], [8]. However, the $x-y$ inhomogeneity problem has not been properly examined to its full extent, as the previous LC unit cells did not have to face this variation. Most of the cells in the literature do have an $x-y$ variation, but assuming that the LC of the whole cavity is equally polarized results in negligible errors. This is because the regions where this assumption does not hold do not have a strong RF relevance, as the RF electric field is confined only below the metallic elements.

However, in the unit cells proposed in this work, the RF electric field of both polarizations must be considered, and the volumes underneath the dipoles will, in general, have different LC states. Therefore, to consider an accurate LC state in those regions, a strategy to account for $x-y$ inhomogeneity in an efficient way must be introduced. The proposed solution consists on splitting the LC region in two sub-volumes, one per each polarization, and considering two different permittivity tensors. However, defining the boundary of each volume requires to look at the AC electric field of the cavity in different biasing scenarios, especially where the interactions between the different LC states are greater. The methodology to determine these two LC sub-volumes is shown in Fig. 5. The AC electric field of the region of interest, in which a boundary of the sub-volume must be defined, is shown in Fig. 5a for several pairs of biasing voltages (cut plane at $y = 1.2mm$). For the sake of brevity, only the AC field in one of the boundaries (red region of Fig. 5b) is shown in Fig. 5a. Considering such AC electric field, the boundary is placed where the interaction between both metallizations is lowest ($x = 0.972mm$). Similarly, the other region where the interaction can be strong, is also analyzed, resulting in a boundary in $x = 0.085mm$, thus defining the X-polarization LC sub-volume block. The Y-polarization block is then defined as the subtraction between the period and the defined block (X-pol). The resulting LC blocks are shown in Fig. 5b. Once the two blocks are defined, the averaged E-field is used to compute the corresponding effective homogeneous tensor. This enables a fast but accurate simulation of the unit cells in all the voltage state pairs in periodic environment. The phase-shift resulting from this partition strategy has been compared with a finer grained partitioning where only the regions below the metallic elements are switchable, with very little discrepancy between both but resulting in a lower computation time.

D. Unit Cell Results

Fig. 6 shows the simulated unit cell reflection coefficient for different pairs of LC states using the aforementioned model. The voltage sweep is $V = V_x$ for X-Pol ($V_y = 0$) and $V = V_y$ for Y-Pol ($V_x = 0$). Thanks to the final dimensional fine tuning in the unit cell design, the maximum cross-polarization level of the unit cell reflection coefficient (S_{XY} and S_{YX}) across all the bias states is -12dB.

The unit cell tolerance to different incidence angles has been tested (Fig. 7). As expected, due to the small period and high symmetry of the unit cell, changing the incidence angle has a very limited effect on the reflection coefficient. In the figure, the S_{YY} is shown for $V_y = 0V$ and $V_y = 5V$ ($V_x = 0$) under different incidence angles.

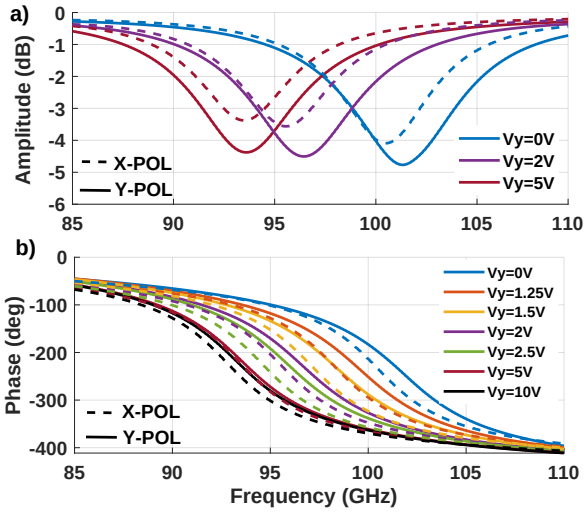

Fig. 6. S_{XX} and S_{YY} reflection coefficients as a function of the frequency. a) Amplitude b) Phase.

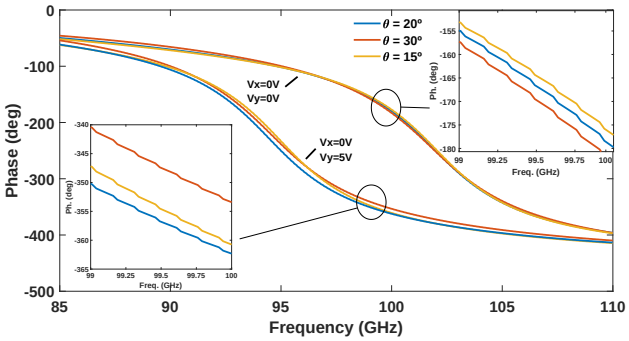

Fig. 7. S_{YY} phase under different incidence angles for two LC biasing states.

III. Dual Polarization LC Antenna Design

With the previously proposed unit cell, an electrically large reflectarray antenna capable of beam steering in two orthogonal linear polarizations is designed. The reflectarray surface contains a quasi-periodic array of 55×55 elements whose structure can be seen in Fig. 1, and the focal points for the two polarizations are chosen to be at $(x_f, y_f, z_f) = (31.3, 0, 136)mm$. The unit cells are simulated in a periodic environment. A simulation is carried out for each of the different incident angles and pairs of biasing voltages, in order to obtain the S-parameter matrix in each case. Then, considering the impinging electric field from the feed, and the desired S-parameters for a specific radiation pattern, the reflected field on the aperture is computed in each unit cell.

The gain radiation pattern cuts in the scanning plane can be observed in Fig. 8. As can be seen, each polarization behaves very similarly when pointing towards different directions between 5º and 40º. The maximum gain is 25dBi and the corresponding efficiency is of 24%. It must be mentioned that the scanning region from 5º to negative angles suffers from blockage of the feeding. However, if the distortion and gain reduction due to the scattering on these elements are assumed, the scanning range could be drastically increased. The time response of the antenna is in the order of the seconds.

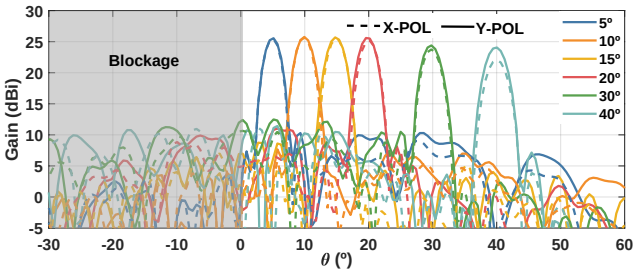

Fig. 8. X-Pol and Y-Pol radiation patterns at 98GHz.

IV. Conclusion

A dual-polarization LC-based reconfigurable reflectarray antenna operating at W-band is proposed in this work. Two novel unit cells, a single-resonant one and a multi-resonant one, have been designed such that different LC states can control independent polarizations within the same cell and single LC cavity, which represents a considerable complexity reduction with respect to the state of the art. It has been shown that the LC can be locally tuned while maintaining low the coupling between polarizations, which is not evident in anisotropic materials. A study is carried out to minimize the impact of introducing the LC bias lines in the cells, after which the single-resonant cell has been chosen for a complete design. Together with the proposed cell, an analysis strategy has been developed to model it accurately. The antenna is capable of beam-steering over one plane from 5º to 40º, with a maximum gain of 25dBi and an SLL as low as -9dB. A prototype is being manufactured and the corresponding measurements will be presented at the conference.

References

[1] S. Bildik, S. Dieter, C. Fritzsch, W. Menzel, and R. Jakoby, "Reconfigurable folded reflectarray antenna based upon liquid crystal technology," *IEEE Transactions on Antennas and Propagation*, vol. 63, no. 1, pp. 122–132, 2015.

[2] G. Perez-Palomino, P. Baine, R. Dickie, M. Bain, J. A. Encinar, R. Cahill, M. Barba, and G. Toso, "Design and experimental validation of liquid crystal-based reconfigurable reflectarray elements with improved bandwidth in f-band," *IEEE Transactions on Antennas and Propagation*, vol. 61, no. 4, pp. 1704–1713, 2013.

[3] G. Perez-Palomino, M. Barba, J. Encinar, R. Cahill, R. Dickie, and P. Baine, "Liquid crystal based beam scanning reflectarrays and their potential in satcom antennas," in *2017 11th European Conference on Antennas and Propagation (EUCAP)*, pp. 3428–3431, 2017.

[4] H. Kim, J. Kim, and J. Oh, "Liquid-crystal-based x-band reactively loaded reflectarray unit cell to reduce reflection loss," *IEEE Antennas and Wireless Propagation Letters*, vol. 20, no. 10, pp. 1898–1902, 2021.

[5] W. Zhang, Y. Li, and Z. Zhang, "A reconfigurable reflectarray antenna with an 8 μm-thick layer of liquid crystal," *IEEE Transactions on Antennas and Propagation*, vol. 70, no. 4, pp. 2770–2778, 2022.

[6] H. Kim, S. Oh, S. Bang, H. Yang, B. Kim, and J. Oh, "Independently polarization manipulable liquid- crystal -based reflective metasurface for 5g reflectarray and reconfigurable intelligent surface," *IEEE Transactions on Antennas and Propagation*, vol. 71, no. 8, pp. 6606–6616, 2023.

[7] G. Perez-Palomino, R. Florencio, J. A. Encinar, M. Barba, R. Dickie, R. Cahill, P. Baine, M. Bain, and R. R. Boix, "Accurate and efficient modeling to calculate the voltage dependence of liquid crystal-based reflectarray cells," *IEEE Transactions on Antennas and Propagation*, vol. 62, no. 5, pp. 2659–2668, 2014.

[8] R. Guirado, G. Perez-Palomino, M. Ferreras, E. Carrasco, and M. Caño-García, "Dynamic modeling of liquid crystal-based metasurfaces and its application to reducing reconfigurability times," *IEEE Transactions on Antennas and Propagation*, vol. 70, no. 12, pp. 11847–11857, 2022.